*lubricants*

MDPI

*Article*

# Sonochemical Synthesis of CuO Nanoplatelets and Their Tribological Properties as an Additive in Synthetic Oil Using Reciprocating Tribometer

**Siraj Azam [1] and Sang-Shin Park [2,*]**

[1] Department of Mechanical Engineering, Yeungnam University, Gyeongsan 38541, Republic of Korea; sirajazam@gmail.com
[2] School of Mechanical Engineering, Yeungnam University, Gyeongsan 38541, Republic of Korea
* Correspondence: pss@ynu.ac.kr

**Abstract:** This Research aimed to improve the tribological properties of commercially available lubricating oil (5W-40) by incorporating CuO nanoplatelets (NPs) synthesized using a simple and cost-effective sonochemical method. To evaluate the performance of the nanolubricant, a reciprocating tribometer was indigenously designed and developed to measure the coefficient of friction (COF) and wear tracks between two AISI 1045 steel surfaces. The CuO NPs were characterized using XRD to confirm their purity and phase, while SEM and FE-TEM were utilized to study their morphology and composition. Raman spectroscopy was used to reveal three distinct Raman active peaks of CuO at 283, 330, and 616 $cm^{-1}$. Zeta potential measurements demonstrated good dispersion quality, with a value of 92.0 mV for 0.1% concentration. SEM and FE-TEM analysis of the nanolubricant showed the formation of a tribo-film over the CuO NPs and adding 0.1% CuO NPs reduced COF by 32%. These findings suggest that incorporating synthesized CuO NPs in commercially available lubricating oil can enhance its tribological properties, leading to improved machine efficiency and lifespan, as well as reduced energy demand. Overall, the study demonstrates the potential benefits of using CuO nanoplatelets as an additive in lubricating oil, which could have significant implications for the development of more efficient nanolubricants.

**Keywords:** nanolubricants; copper oxide; reciprocating tribometer; spectroscopy; data acquisition



**Citation:** Azam, S.; Park, S.-S. Sonochemical Synthesis of CuO Nanoplatelets and Their Tribological Properties as an Additive in Synthetic Oil Using Reciprocating Tribometer. *Lubricants* **2023**, *11*, 185. https://doi.org/10.3390/lubricants11040185

Received: 7 April 2023
Revised: 20 April 2023
Accepted: 20 April 2023
Published: 21 April 2023



## 1. Introduction

Tribology is a field of study that focuses on the interactions between surfaces in relative motion, encompassing friction, wear, and lubrication. In manufacturing industries, friction and wear are critical factors that can significantly affect the performance and lifespan of machine parts. High levels of friction can cause wear and tear, leading to decreased efficiency and even complete machine failure. This can result in costly repairs, production downtime, and decreased productivity. Therefore, reducing friction and wear is of paramount importance in the manufacturing industry. Lubrication plays a crucial role in reducing friction and wears between interacting surfaces. The primary function of a lubricant is to create a protective layer between two metal surfaces, reducing friction and inhibiting wear. The effectiveness of a lubricant depends on its chemical and physical properties, such as viscosity, load-carrying capacity, and thermal stability. Therefore, enhancing the properties of lubricants can lead to improved efficiency and an extended lifespan of machine parts, resulting in increased productivity and reduced costs. Research in tribology has been focused on developing new and advanced lubricants that can overcome the challenges of high friction and wear in manufacturing industries. These lubricants can be designed to have tailored properties that meet specific requirements, such as high-temperature stability, low volatility, and biodegradability. Nanoparticles, such as CuO, $TiO_2$, and $MoS_2$, have also been used as additives to enhance

lubricant performance by forming a protective tribo-film on metal surfaces, reducing friction and wear. Several approaches have been proposed to achieve this goal, including the addition of nanoparticles and other additives to lubricating oils. These strategies aim to improve the tribological properties of the lubricant, leading to reduced energy losses, increased efficiency, and improved productivity. Jingfang Zhou et al. [1], after performing electron probe microanalysis (EPMA) and X-ray photoelectron spectroscopy (XPS) on the rubbed surface, it was determined that the boundary film of the worn surface consisted of two layers: a Cu nanoparticle film that was deposited and a tribo-chemical reaction film containing S and P. The effective tribological properties of the oil were attributed to a collaborative effect between these two layers. Raimondas et al. [2] argued that the friction pair comprising aluminum and steel exhibited more uniform friction. The primary cause behind the reduction in friction and wear was believed to be the existence of an adsorption layer. Xiong et al. [3] showed that the incorporation of $WO_3$:$Eu^{3+}$ in water-based lubricants led to a significant enhancement in load-carrying capacity, wear resistance, and reduction of friction. Yuefeng Du et al. [4] showed the scanning electron microscope (SEM) images revealed that AGEC's worn surface had a dense graphene self-lubricant film, which contributed to its superior tribological performance. Therefore, this study proposes a path to widen the scope of tribological applications of graphene-epoxy composites based on the outstanding tribological properties of AGEC. Johan Guegan et al. [5] have reported the synergistic and antagonistic effect of various friction modifier additives to reduce friction. Recently, nanoparticles have been used as an additive in lubricants. Various studies have proposed the use of nanoparticles for the reduction of friction and wear losses caused by damage on a surface. Many application-based types of research propose the use of nanoparticles as an additive to reduce COF. B.S. Shenoy et al. [6] showed that the load-carrying capacity increased by using nanoparticles. Zhao et al. [7] investigated the impact of different types of CuO nanostructures on the tribological properties of water-based lubricants as an additive, utilizing a UMT-2 micro-friction tester. Moreover, they delved into the underlying mechanisms that contribute to these properties. Ahmed A et al. [8] proposed that the use of copper oxide as a nano additive indicates an improvement in tribological properties, resulting in a decrease in friction coefficient by 14.59% to 42.92% when compared to the original lubricant. Shafi et al. [9] proposed nanoparticles have the potential to be used as lubricant additives, offering significant benefits over the organic molecules currently utilized. Their minute size allows them to penetrate the contact area with ease, resulting in a reduced real contact area when they become entrapped between mating surfaces. Furthermore, they are typically effective even at ambient temperatures. Shui-quam Huang et al. [10] study systematically examined the friction and wear properties of water-based nanolubricants using a block-on-ring testing setup with a contact pair consisting of stainless and alloy steel. The concentration and mass ratio of nano additives were adjusted in the range of 0.02 to 0.10 wt% and 1:5 to 5:1, respectively, to achieve the best lubrication performance. Tuyana Dembelova et al. [11] examined the impact of incorporating silicon dioxide nanoparticles as a nano-additive on the performance characteristics of polyethylsiloxane lubricant. The findings indicated an enhancement in the tribological properties of the lubricant, as evidenced by an increased tear strength of the lubricating film and a corresponding improvement in the friction coefficient with increasing sliding speed. A range of microscopy techniques was employed in this study to examine the surface properties and lubricating mechanisms in Kinjal Trivedi [12] work. The differences in molecular structure and nanoparticle stability between the two oils were deemed responsible for the results obtained. Bader Alqahtani et al. [13] suggest that, to compare the thermal conductivity and flashpoint of the base oil and nanofluid-added 5W30 lubricant, kinematic viscosity was computed. The incorporation of nano-additives resulted in a 15% improvement in wear scar and a 33% improvement in coefficient of friction. Adam Rylski et al. [14] demonstrated the impact of $ZrO_2$ nanoparticle agglomeration on the frictional properties of lithium grease. The incorporation of 1

wt% $ZrO_2$ nanoparticles into the pure lithium grease lead to a significant reduction in the friction coefficient, reaching up to 50%. The experimental tribological investigation of a nanosized ceramic mixture composed of yttria and zirconia as an engine lubricant additive is presented in Adam I. Szabo et al. [15] study. The ceramic mixture was formulated using yttria-stabilized zirconia (YSZ) nanoparticles, with a weight ratio of 11:69 of yttria to zirconia. Based on the ball-on-disc tribological measurements, the optimal concentration was determined to be 0.4 wt%, which led to a reduction of 30% in wear diameter and 90% in wear volume at the same coefficient of friction. Padgurskas et al. [16] used Fe, Cu, and Co nanoparticles to examine the tribological properties of lubricants. Prabu et al. [17] have shown the influence of Ag nanoparticles in mineral oil to reduce wear properties. Jingfang Zhou et al. [1] have discussed the role of Cu nanoparticles in oil in modifying the tribological behavior of lubricating oil. Shahnazar et al. [18] have reported the use of $TiO_2$, ZnO, and $ZnAl_2O_4$ nanoparticles for enhancing lubricant properties. Laad et al. [19] proposed $TiO_2$ nanoparticles as an additive in engine oil. Dai et al. [20] listed many nanoparticles used as an additive in lubricants. CuO nanoparticles have also been used as an additive in the field of tribology. To analyze and enhance the tribological properties of a lubricant, Alves SM et al. [21] showed the prospect of reducing the COF using tiny CuO nanoparticles. Gulzar et al. [22] used CuO and $MoS_2$ for improving the anti-wear properties of lubricating oil. Peña-Parás et al. [23] showed the effect of CuO nanoparticles on the wear surface diameter using Polyalphaolefin (PAO) oil and the effect of $Al_2O_3$ on tribological properties. Hernández Battez et al. [24] showed that the deposition of CuO, ZnO, and $ZrO_2$ nanoparticles on the wear surface led to the best results compared to the deposition of other nanoparticles. Gupta et al. [25] carried out the surface modification of CuO nanoparticles for load-carrying capacity and COF reduction was also demonstrated. Thottackkad et al. [26] reported that the frictional force and wear rate decrease with an increase in the concentration of CuO nanoparticles using engine oil as a lubricant (SAE 15W-40). Nevertheless, several investigations conducted by researchers failed to determine the optimal weight percent concentration of additives required in lubricating oil. Furthermore, most of these studies utilized commercially available CuO nanoparticles, which often exhibit a generally spherical morphology and suboptimal dispersion quality.

Various types of tribometers are used to measure the COF, such as pin-on-disc [19,26–30], four-ball tester [17,25,31], and high-frequency reciprocating ring (HFRR) tribometer [32,33], etc. The measurement of the coefficient of friction (COF) of lubricating fluids is a crucial aspect of tribology, and pin-on-disc tribometers are widely used for this purpose. However, one of the challenges associated with pin-on-disc tribometers is the difficulty in maintaining perpendicularity between the pin and the disc due to the uni-directional rotational motion. The rotation of the disc generates torque in the direction of motion, causing a bend in the pin, which results in the loss of perpendicularity. Reciprocating tribometers, on the other hand, have a back-and-forth motion that does not allow the pin to bend in one direction, making it easier to maintain perpendicularity between the pin and the reciprocating plate. As a result, reciprocating tribometers are more stable and precise for measuring the COF than pin-on-disc tribometers. In addition, the fabrication cost of the reciprocating tribometer is comparatively low, making it a more feasible option for laboratory experiments. Therefore, in this research we adopted the use of reciprocating tribometers to study the tribological properties of lubricating fluids.

This study aimed to improve the tribological properties of SAE (5W-40) fully synthetic oil by adding CuO nanoplatelets (NPs) synthesized through a simple and cost-effective sonochemical method. The concentration of CuO NPs in the lubricating oil was optimized to achieve high dispersion quality using a reciprocating tribometer. This was done to obtain the coefficient of friction (COF). This study reports excellent dispersion of CuO NPs in lubricating oil. This is a significant development that may be exploited in commercial applications to further enhance lubricant's tribological properties. By improving the tribological properties of lubricating oils, machines' efficiency, and lifespan can be

increased, while energy consumption can be decreased. Therefore, this research provides a promising solution to overcome friction and wear challenges, especially in producing effective nanolubricants.

## 2. Materials and Methods

### *2.1. Synthesis of CuO NPs*

CuO nanoparticles have been synthesized using diverse strategies, such as solid-state thermal decomposition [34], the colloid microwave-thermal method [35], solid-state reaction method [36], sol-gel method [37], gel combustion method [38], etc. In the present study, CuO nanoparticles were synthesized using a sonochemical technique with copper nitrate [Cu $(NO_3)2.3H_2O$] and ammonia solution ($NH_3$) without any surfactant or templates. High purity chemicals were purchased from Sigma Aldrich and used without further purification. The synthesis involved dispersing a stoichiometric amount of copper nitrate [Cu $(NO_3)2.3H_2O$] in 100 mL of deionized water, subjecting it to ultrasonic radiation for 30 min, and adding $NH_3$ dropwise to the solution resulting in the formation of a precipitate. The pH was maintained at 9, and the solution was subjected to ultrasonic radiation again to turn the precipitate black. The black precipitate was collected, washed with water and ethanol using a centrifuge at 3000 rpm, dried in an oven at 80 °C for 24 h, and calcinated at 400 °C for 2 h, resulting in the formation of CuO NPs. The synthesis process of CuO nanoparticles is shown in Figure 1. The structural characterization of the synthesized CuO NPs was done using an X-ray diffractometer (PANalytical, X'Pert PRO) with Cu-Kα radiation, and the Raman spectrum was obtained using a Raman microscope (Horiba, Xplora Pluse) having an excitation source of 532 nm laser at a power of 8 mW. The morphology of the nanoparticles was analyzed by SEM (Hitachi, S-4800) and FE-TEM (Tecnai G2 F20 S-TWIN). The characterization of the synthesized nanoparticles (NPs) was performed using scanning electron microscopy (SEM) with energy dispersive spectroscopy (EDS) and field emission transmission electron microscopy (FE-TEM). Zeta potential measurements were conducted using a Nano Zetasizer (Malvern, Nano ZS ZEN3600), while the coefficient of friction (COF) was measured using a reciprocating tribometer that was developed in the lab.

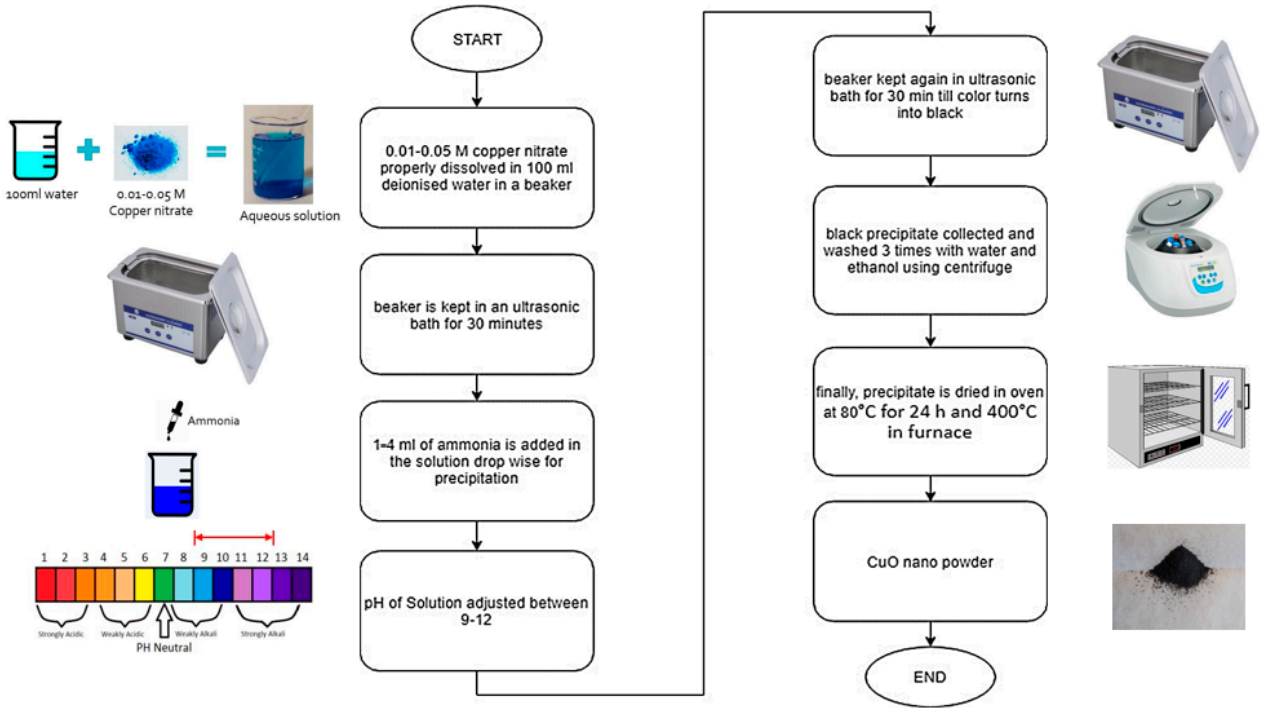


**Figure 1.** Synthetization of CuO Nanoparticles.

### 2.2. Design and Setup

Figure 2 depicts the schematic diagram of an indigenously designed and fabricated reciprocating tribometer with the dimensions of the pin and plate used for the test. The tribometer comprises two air-linear guides mounted on a rail, which moves horizontally to produce reciprocating motion. The reciprocating plate and 12 V DC motor are attached to the screw guide, which is in turn attached to the ball joint bolt and load cell. When the motor rotates, it converts rotational motion into reciprocating motion, pushing the load cell attached to the reciprocating plate. The air compressor supplies pressurized air between the linear guides and the rail, generating an air gap of approximately 2 µm. The air gap keeps the linear guides and rail apart from each other, which helps to maintain no friction between the two parts. Therefore, a pure force can be acquired between the pin and the reciprocating plate as shown in Figure 2. Fx represents the tangential force generated on the reciprocating plate, and Fy represents the normal force generated from the applied load on the pin. The coefficient of friction (µ) can be calculated using Fx and Fy.

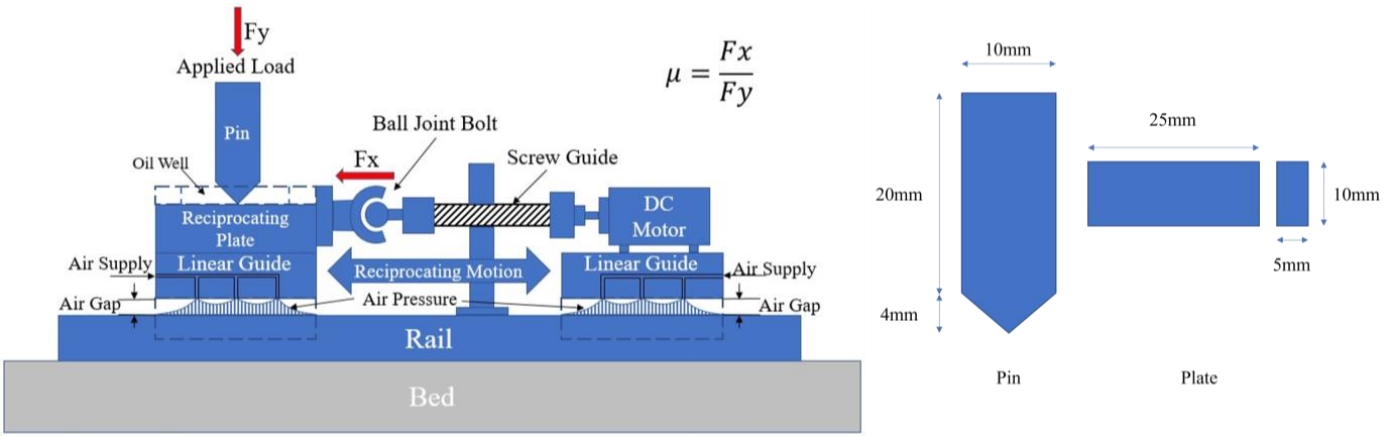


**Figure 2.** Schematic diagram of reciprocating tribometer and dimensions of pin and plate.

Figure 3 illustrates the assembly of the experimental and data acquisition setup. The 12 V DC motor is connected to the L298N driver and Arduino board, which controls its direction of motion to produce reciprocating motion on the horizontal plate. Two limit switches are mounted on the bed to control the direction of motion. When touched by the linear guide, they change the rotation of motion in the opposite direction. The Arduino program is designed to control the DC motor with the limit switches and to acquire the data of Fx and Fy forces from the two load cells attached as shown in Figure 3. The program is also designed to start data acquisition one second after the motor starts and stop collecting data one second before when the motor is going to change its direction. This is necessary to avoid errors produced due to changes in the motor's acceleration when changing direction. The data of Fx and Fy forces are collected only when the motion is in the forward direction, neglecting the negative force produced during the backward motion. This strategy allows the acquisition of data without any errors, making the calculation of COF more accurate and convenient. The pin and sliding plate are made of AISI 1045 steel. The motor generates a rotational motion of 380 rpm, giving the sliding plate a speed of 1.4 m/min according to the pitch of the screw guide. The actual photograph of the reciprocating tribometer is shown in Figure 4.

### 2.3. Preparation of Nanolubricants

In this study, Shell Helix Ultra SEA 5W-40 fully synthetic motor oil was used as the base oil, and its typical physical characteristics are provided in Table 1. Nanolubricants were prepared by combining different weight percentages of CuO nanoplates (NPs) with the base oil in separate 4 mL containers. CuO NPs at concentrations of 0.05, 0.1, 0.15, and 0.2 weight percent were well-mixed and dispersed into the base oil as shown in Figure 5.

To mix the samples, they were placed in an ultrasonic bath for 2 h and subsequently mixed using a vortex mixer.

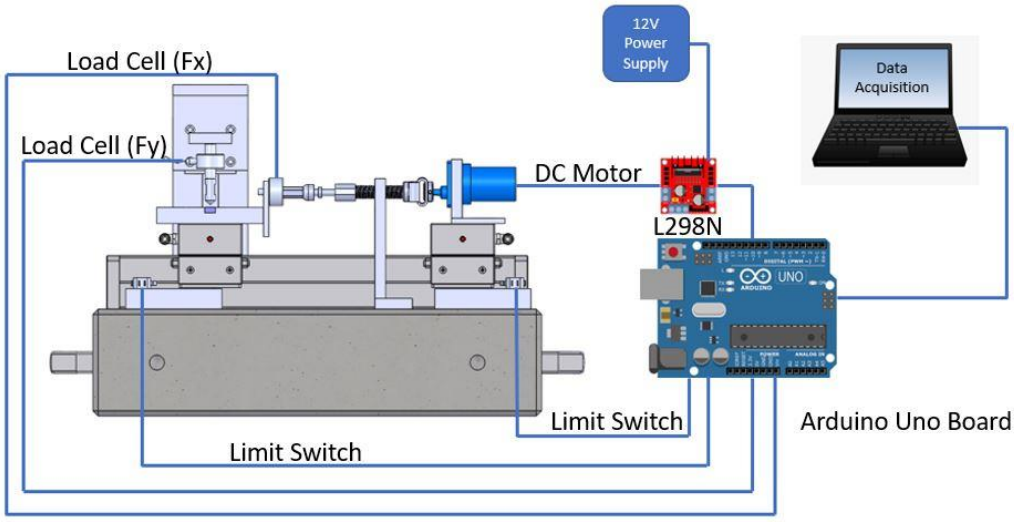


**Figure 3.** Experimental and data acquisition setup.

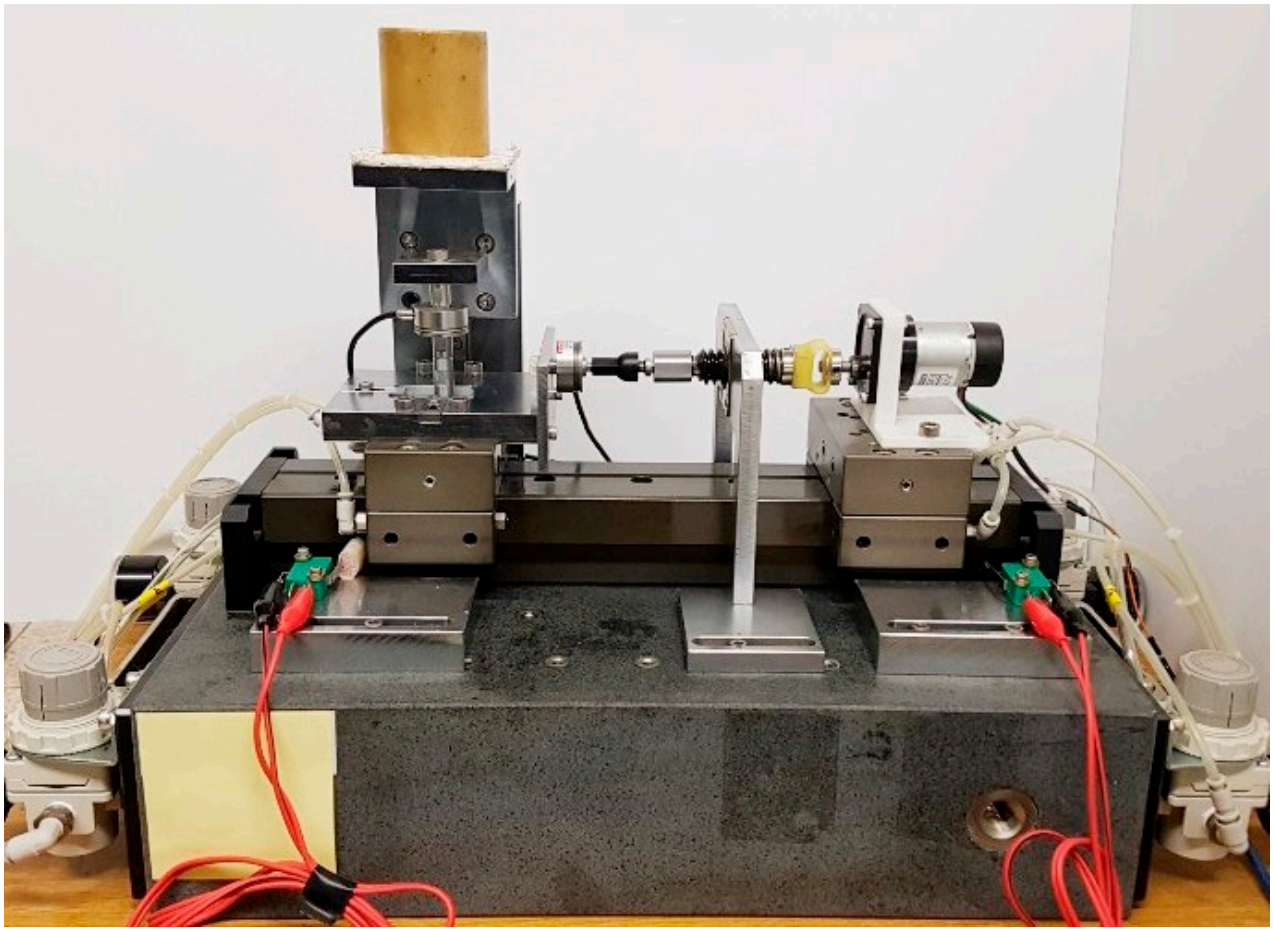

**Figure 4.** Photograph of reciprocating tribometer.

**Table 1.** Typical physical characteristics of base oil.

| Properties | Methods | Shell Helix Ultra 5W-40 |
|---|---|---|
| Viscosity Grade | data | 5W-40 |
| Kinematic Viscosity @40 °C (cSt) | ASTM D445 | 74.4 |
| Kinematic Viscosity @100 °C (cSt) | ASTM D445 | 13.1 |
| Density @15 °C (kg/L) | ASTN 4052 | 0.840 |
| Pour Point (°C) | ASTM D97 | −39 |
| Hths Viscosity @150 °C (m PaS) | ASTM D4741 | 3.68 |
| Flash Point (Pmcc) (°C) | ASTM D93 | 215 |

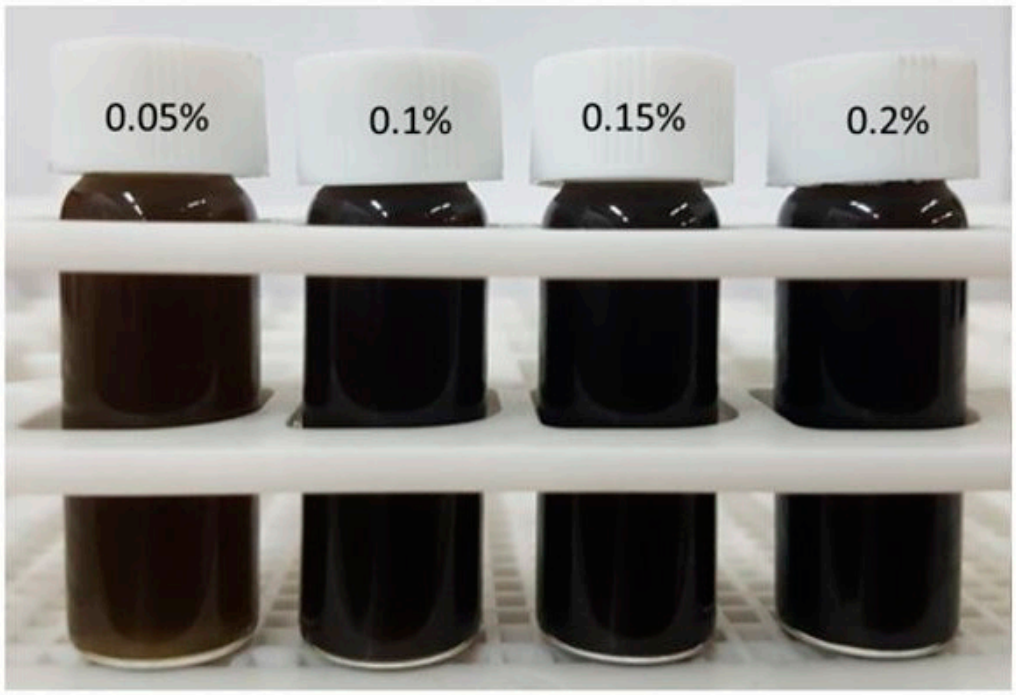


**Figure 5.** Nanolubricant prepared with varying weight percent of CuO NPs.

### *2.4. Testing Conditions*

To obtain similar surfaces and overcome surface irregularities, both the pin and plate were initially sanded using CC-1000Cw sandpaper. Initially, two dry condition tests were performed without oil, and the pin and plate were rubbed against each other at the same speed as in the test using pure oil. The dry condition caused severe damage to the pin and plate; hence the dry condition tests were carried out twice, and the average was taken as a reference. All tests with oil were carried out five times successively for four hours, and the average was calculated for the result. The experimental setup was designed to collect the normal force (Fx) and tangential force (Fy) data after every 15 min of a run. The Fx and Fy data were collected digitally for four hours, and the COF was calculated from this data. The actual experimental parameters are tabulated in Table 2.

**Table 2.** Experimental Parameters.

| Parameters | Value |
|---|---|
| Applied Load | 20 N |
| Speed of motor | 380 rpm |
| Sliding Speed | 1.4 m/min |
| Test Run Time | 4 h |

## 3. Results and Discussions

### *3.1. Structural Characterization*

The XRD pattern presented in Figure 6 confirmed the formation of CuO NPs, with well-defined and intense peaks (110), (002), (111), (−202), (020), (202), (−113), (−311) corresponding to diffraction angels 32.48°, 35.49°, 38.80°, 48.84°, 53.52°, 58.36°, 61.63°, 66.33° respectively. These peaks were in good agreement with the standard values (JCPDS 80-1268) and established the monoclinic structure of CuO NPs. Further, the purity of the sample was established based on the absence of any impurity peaks in the XRD pattern. The crystallite size of the CuO NPs was calculated using the well-known Scherrer's equation ($D = \frac{0.9\lambda}{\beta cos\theta}$) and the average crystallite size was estimated to be 100 nm.

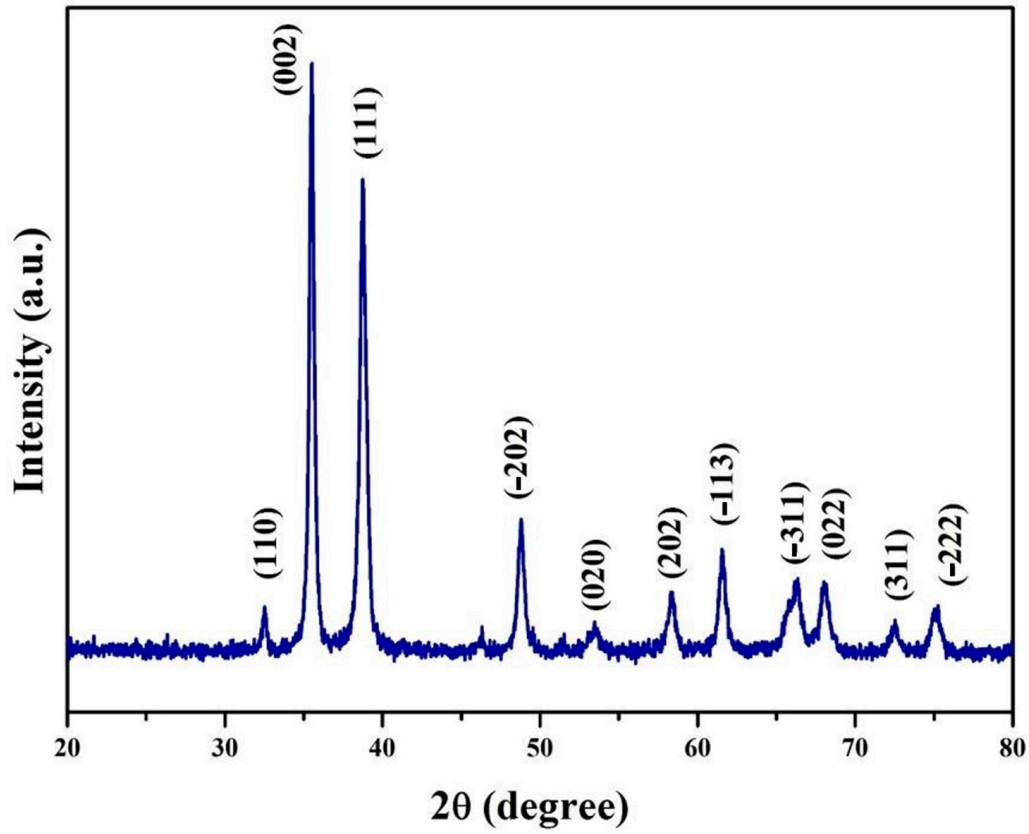


**Figure 6.** XRD pattern of CuO NPs.

Raman spectroscopy is a very important and powerful technique to study and describe the phases and structures of oxides and other systems. With decreasing crystallite size the Raman frequency can shift and broaden the bandwidth. The results obtained from the Raman spectroscopy are plotted in Figure 7. The structure of CuO belongs to a monoclinic crystal system with space group $C^6_{2h}$ having two molecules per unit cell. In the CuO crystal structure, there are nine optical phonon modes and only three modes ($A_g$ and two $B_g$) modes are Raman active. It can be seen clearly from Figure 7 that the well-intense peak at 283 $cm^{-1}$ belongs to $A_g$ mode and the other two peaks at 330 and 616 $cm^{-1}$ belong to $B_g$ mode corroborating the formation of CuO NPs.

### *3.2. Morphological Characterization*

The morphology of the CuO NPs was examined using FE-SEM and FE-TEM. SEM micrographs depicted in Figure 8 shows the presence of nanoplatelets (NPs) of varying sizes, the scale of the SEM image was used as 1 μm and 500 nm. The thickness of the NPs ranges from 52 nm to 66 nm and the width ranges from 200 nm to 400 nm. Some NPs are stacked up while some are lying down as shown in Figure 8a–d. EDS of the CuO NPs

in Figure 8e shows the presence of copper (Cu) and oxygen (O), confirming the purity of the prepared samples. Figure 9a,b shows the results obtained from the FE-TEM depicting the distinct images of CuO NPs similar to the SEM images the scale used in FEM images are 0.5 µm to 100 nm. The EDS and mapping in Figure 9c acquired from the TEM show the presence of Cu and O which can be confirmed from the mapping images showing the orange color of Cu and green color of O.

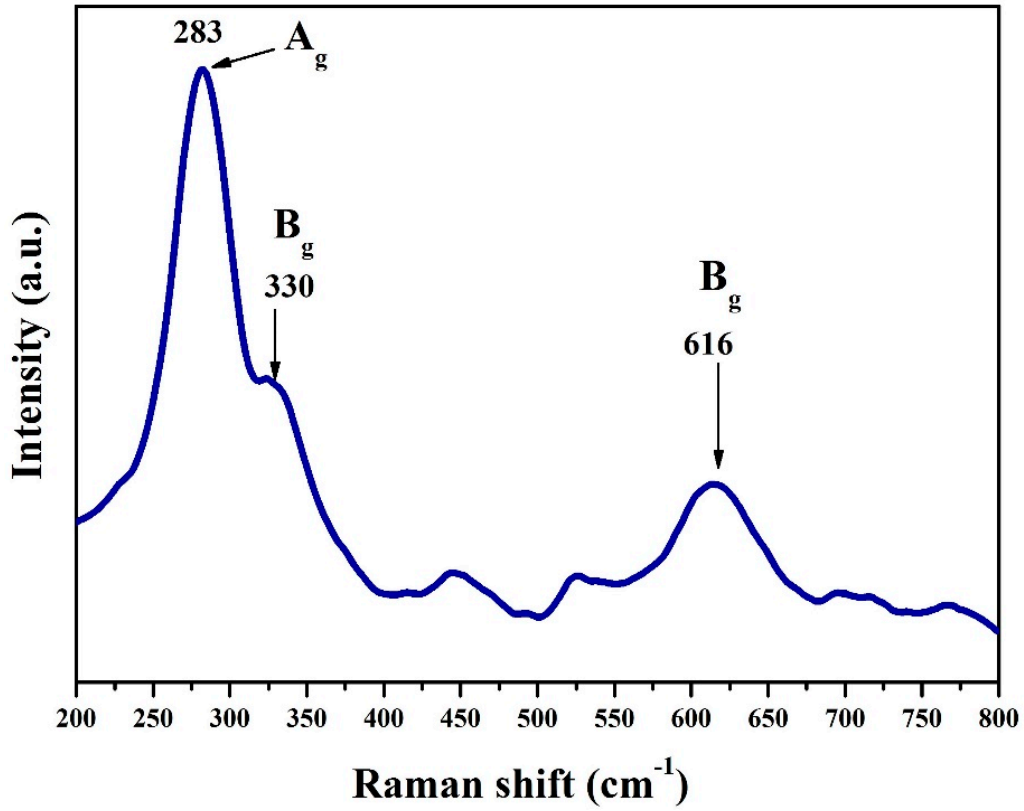


**Figure 7.** Raman spectra of CuO NPs.

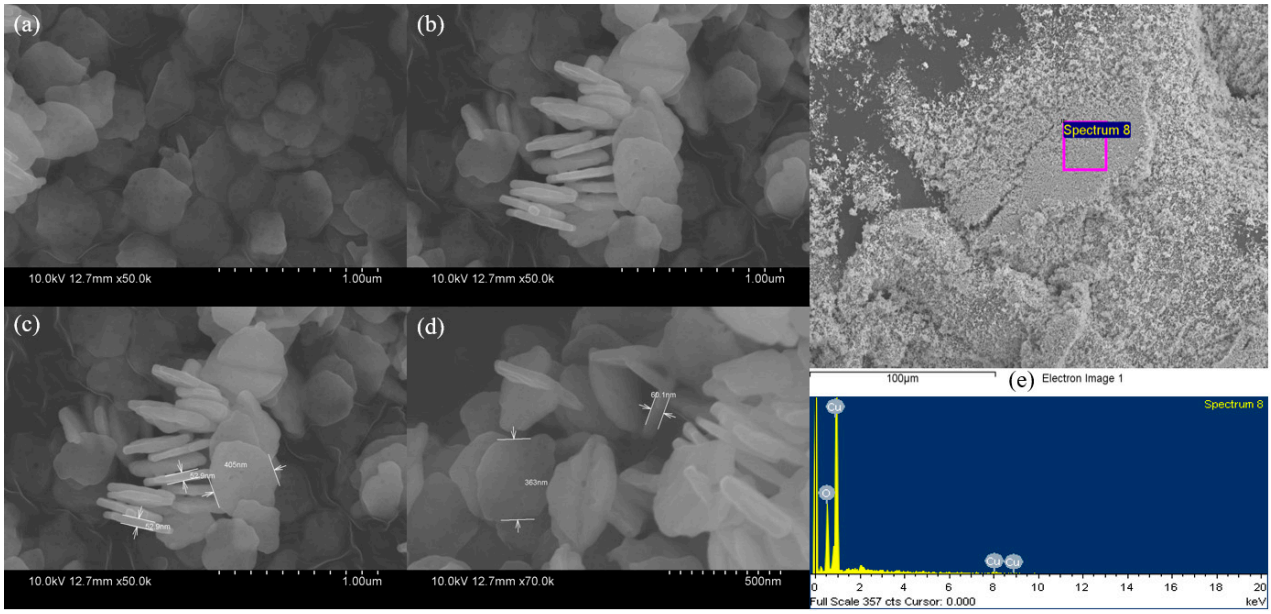


**Figure 8.** (**a**–**d**) SEM images and (**e**) EDS of CuO NPs.

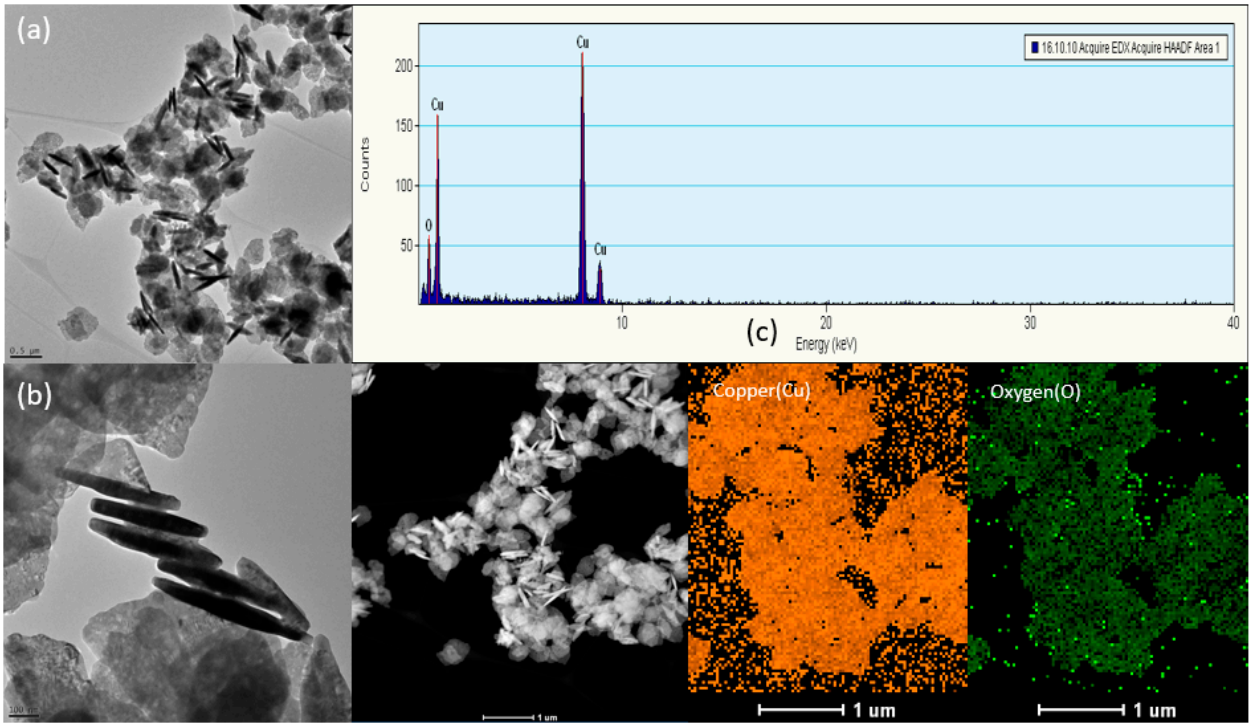


**Figure 9.** (**a**,**b**) FE-TEM images and (**c**) EDS and mapping of CuO NPs.

### *3.3. Effect on Morphology after Mixing in Oil*

After mixing CuO NPs in the lubricating oil, the nanolubricant was characterized using FE-SEM and FE-TEM to determine whether any changes occurred in the shape and size of the NPs after ultrasonication and dispersion in the lubricating oil. For SEM analysis, an Indium tin oxide (ITO) coated glass slide was used, and a small drop of the oil mixed with CuO NPs (nanolubricant) was placed on the charged side of the ITO glass. Subsequently, the ITO glass was placed on a hot plate at 350 °C for about 4 h. Consequently, the oil evaporated from the surface, and the NPs were examined. For analyzing the nanolubricant using FE-TEM, a sample was prepared using ethanol. Drops of nanolubricant were mixed well with ethanol for better dispersion, and the solution was dried on the TEM grid for further investigation. Figure 10a shows the prepared sample for SEM of the nanolubricant, and Figure 10b shows the SEM image demonstrating the similar shape and size and the formation of tribo-film over the CuO NPs. EDS in Figure 10c confirmed the presence of Cu and O. These results were further investigated using FE-TEM analysis shown in Figure 11a,b, showing distinct images of CuO NPs. EDS and mapping are shown in Figure 11c confirming the purity of CuO NPs. The mapping shows the orange color of Cu and the green color of O.

### *3.4. Dispersion of Nanoparticles (NPs)*

The dispersion of nanoparticles (NPs) is a crucial factor in the formation of a nanolubricant, as good dispersion is expected to yield better results. Chen et al. [39] listed various dispersion techniques, which show dispersion stability roles, methods for dispersion, and analysis methods. In this study, ultrasonication with vortex mixing was used for the dispersion of NPs. All the samples prepared for the nanolubricant were kept without disturbing for about 15 days to examine sedimentation in the prepared nanolubricant as shown in Figure 12. It was observed that the sample with 0.1% concentration by weight of CuO NPs showed a very less amount of sedimentation compared to the other concentrations of the nanolubricant. The 0.05%, 0.15%, and 0.2% concentrations showed sedimentation of NPs at the bottom of the container, as shown in Figure 12a. To further validate the dispersion quality of CuO nanoparticles at a concentration of 0.1%, additional experiments were con-

ducted. Three new samples were prepared with the same concentration and were allowed to settle for 15 days. Visual observations of the samples were recorded and compared. The results, as shown in Figure 12b, confirmed that the sample with 0.1% CuO nanoparticles exhibited better dispersion, with minimal sedimentation compared to the other samples. In addition to visual observations, zeta potential measurements were conducted using a Malvern ZEN 3600 Nano Zetasizer to further confirm the dispersion quality. Zeta potential is a measure of the electric charge on the surface of nanoparticles, which can indicate their stability and ability to remain dispersed in a liquid medium. The zeta potential values obtained for the 0.1% CuO nanoparticles were analyzed and found to be within an acceptable range, indicating good dispersion quality and stability of the nanoparticles in the lubricating oil. These additional experiments provided further evidence of the optimized dispersion of CuO nanoparticles at a concentration of 0.1% in the lubricating oil, supporting the conclusion that this concentration is suitable for use as an additive in fully synthetic motor oil (SEA 5W-40).

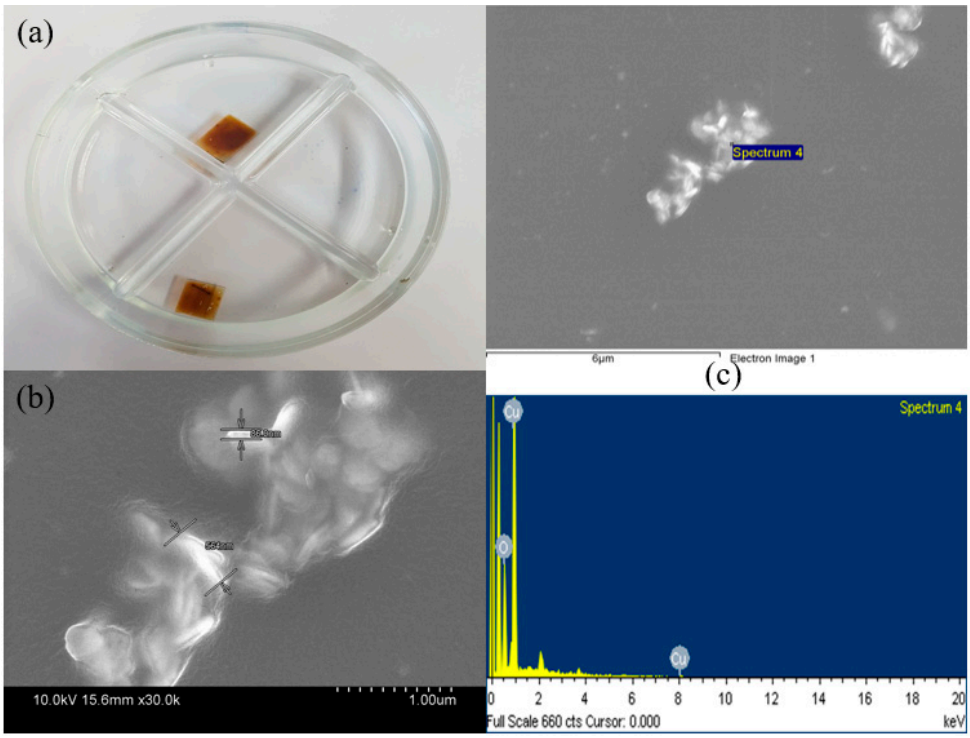


**Figure 10.** (**a**) Samples of nanolubricant on ITO glass; (**b**) SEM image of CuO NPs after mixing in oil; and (**c**) EDS of CuO NPs after mixing in the lubricating oil.

### *3.5. Zeta Potential of Nanolubricants*

Zeta potential analysis gives important information about the quality of dispersions. A high zeta potential provides stability for small molecules and particles, which means the solution or dispersion will resist aggregation. Any colloidal solution with zeta potential above ±60 mV [40] is electrically stable with excellent dispersion. The zeta potential values of 0.05%, 0.1%, 0.15%, and 0.2% concentration of CuO NPs mixed in the lubricating oil were found to be 17.3, 92.0, 24.8, and 48.6 mV, respectively as shown in Figure 13. Interestingly the sample with 0.1% concentration showed the highest zeta potential of 92.0 mV. The visual observation of 0.1% concentration dispersion also showed lesser sedimentation of NPs compared to another weight percent of concentrations as shown in Figure 12 in the previous section. Hence, a 0.1% concentration of CuO NPs is suggested as the optimized value for using them as an additive in fully synthetic motor oil (SEA 5W-40).

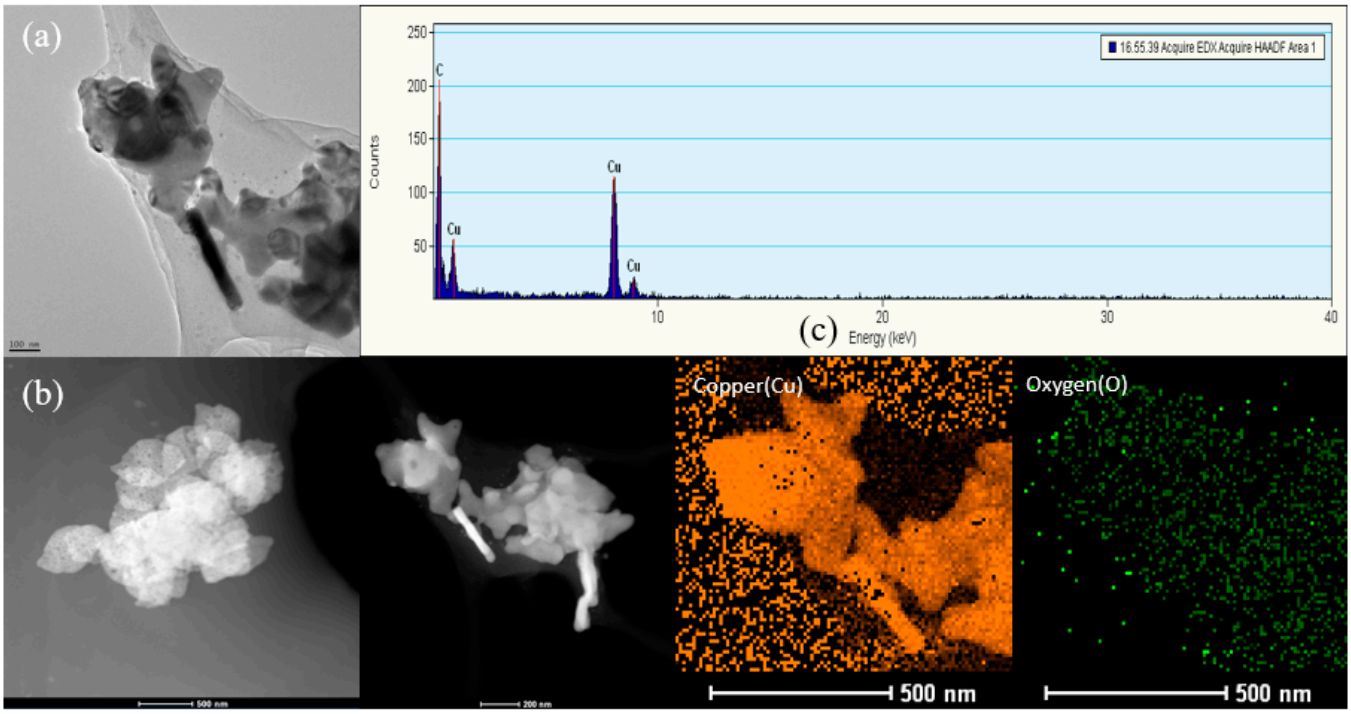


**Figure 11.** (**a**,**b**) FE-TEM images of CuO NPs after mixing in the lubricating oil; and (**c**) EDS and mapping of CuO NPs after mixing in the lubricating oil.

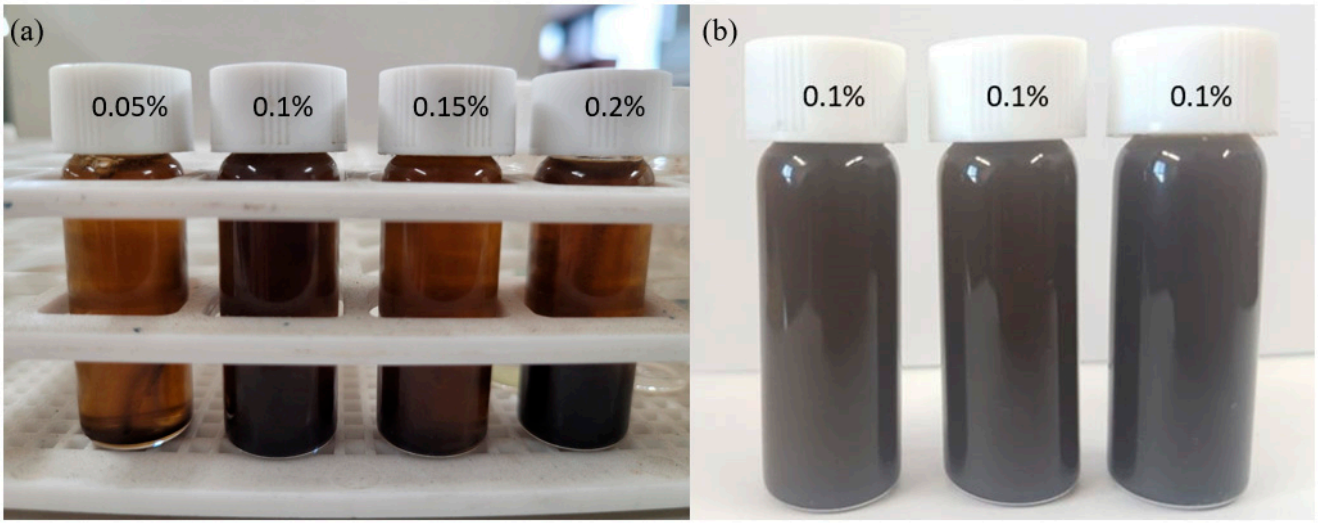


**Figure 12.** Comparison between the sedimentation of NPs after 15 days with (**a**) all samples and (**b**) 0.1% CuO NPs concentration.

### *3.6. Tribological Characterization*

The graph in Figure 14 displays the coefficient of friction (COF) under dry and lubricated conditions. The COF under dry conditions reached a maximum of 0.55 and then decreased to 0.42 after 80 m, with an average of 0.45 up to 300 m. As shown in Figure 14, the COF under lubricated conditions remained almost constant at about 0.2 up to 300 m. This value is quite low compared to the dry conditions. These results confirm that our reciprocating tribometer's functionality matches the standard mechanism of tribometers. Once the functionality of the reciprocating tribometer was confirmed, a nanolubricant was used to investigate the impact of CuO NPs added in four different weight percent concentrations to the lubricating oil on the COF. All tests were conducted successfully at 0.05, 0.1%, 0.15%,

and 0.2% concentrations of CuO NPs in fully synthetic motor oil (SEA 5W-40). The COF values obtained using the nanolubricant were compared with those obtained using pure fully synthetic motor oil (SEA 5W-40), as shown in Figure 15. The standard deviation of the data indicates that the acquired data was widely distributed, ranging from 0.0105 to 0.0099, which represents a low standard deviation. This demonstrates the quality of data acquisition and the tribometer's stability. All tests using the nanolubricant produced better COF values than those using lubricating oil without CuO NPs additives, as shown in Figure 15. The average COF values of pure oil, 0.05%, 0.1%, 0.15%, and 0.2% concentration were found to be 0.194%, 0.155%, 0.131%, 0.166%, and 0.138%, respectively. A 32% reduction in COF was observed when a 0.1% concentration of CuO NPs was added to the lubricating oil. When 0.05%, 0.15%, and 0.2% concentrations of CuO NPs were added to the lubricating oil as an additive, there was a reduction of 20%, 14%, and 28% in COF, respectively. Notably, a 0.1% concentration of CuO NPs as an additive in the lubricating oil (SEA 5W-40) showed the best results in terms of COF. The significant decrease in COF value in the nanolubricants can be attributed to the fact that lubricating oil molecules create a tribo-film along the CuO nanoplatelets, and the nanoplatelets orient themselves in the compressed sliding contact position. This finding is supported by the SEM and FE TEM images of CuO NPs after mixing with lubricating oil, as shown in Figures 10 and 11. Furthermore, good dispersion quality demonstrated a uniform distribution of CuO NPs in lubricating oil, which helps reduce COF. As the dispersion of CuO NPs in the lubricating oil increases, the interface area between CuO NPs and lubricating oil also increases, thereby decreasing friction. This is consistent with the results obtained by Joly-Pottuz et al. [41], who concluded that better dispersion of additives in oil leads to better tribological properties.

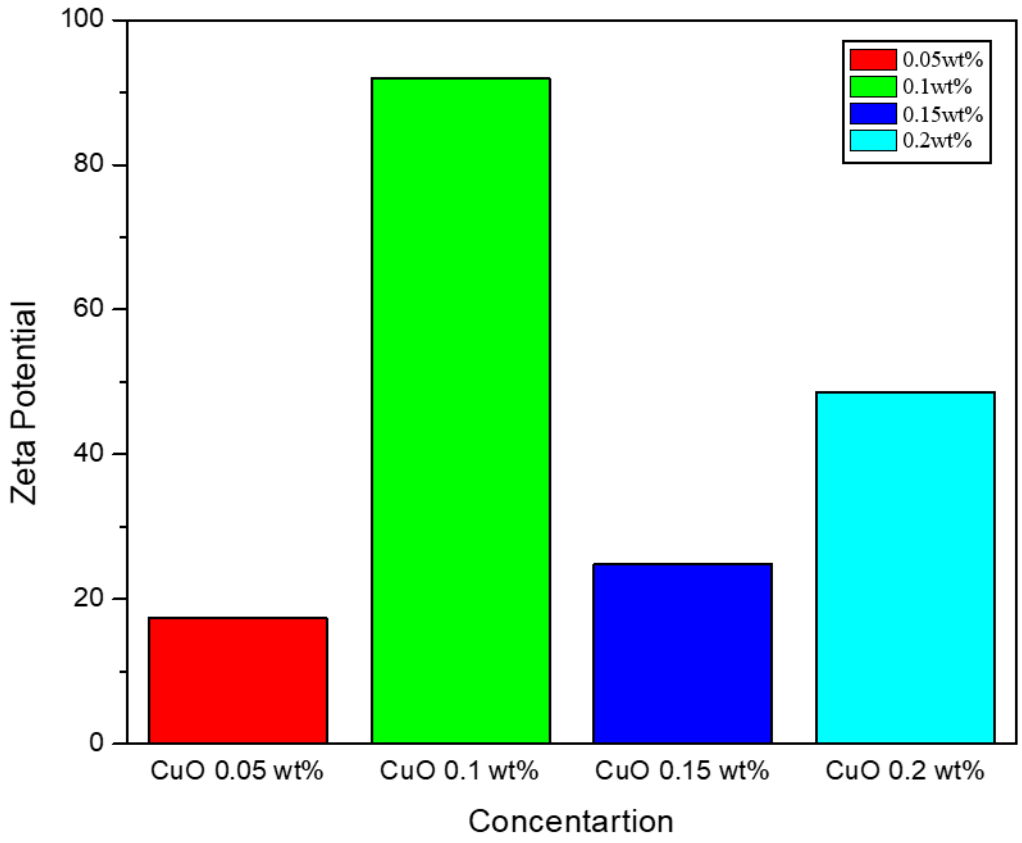


**Figure 13.** Zeta Potential of all concentrations.

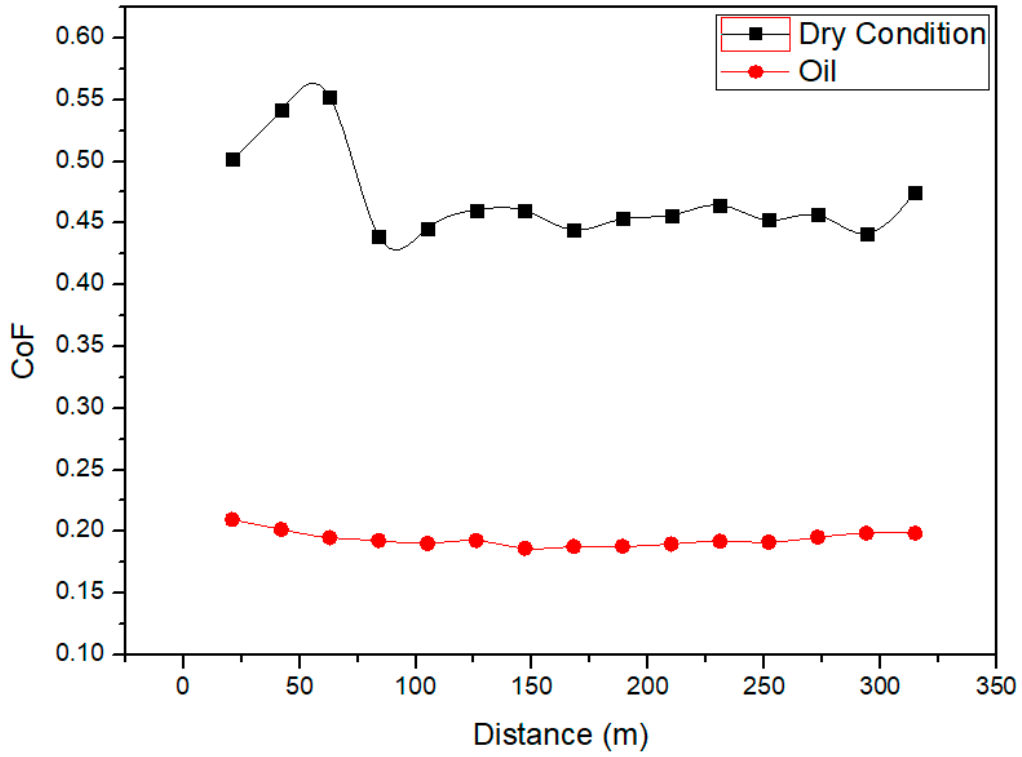


**Figure 14.** COF under dry and pure oil conditions.

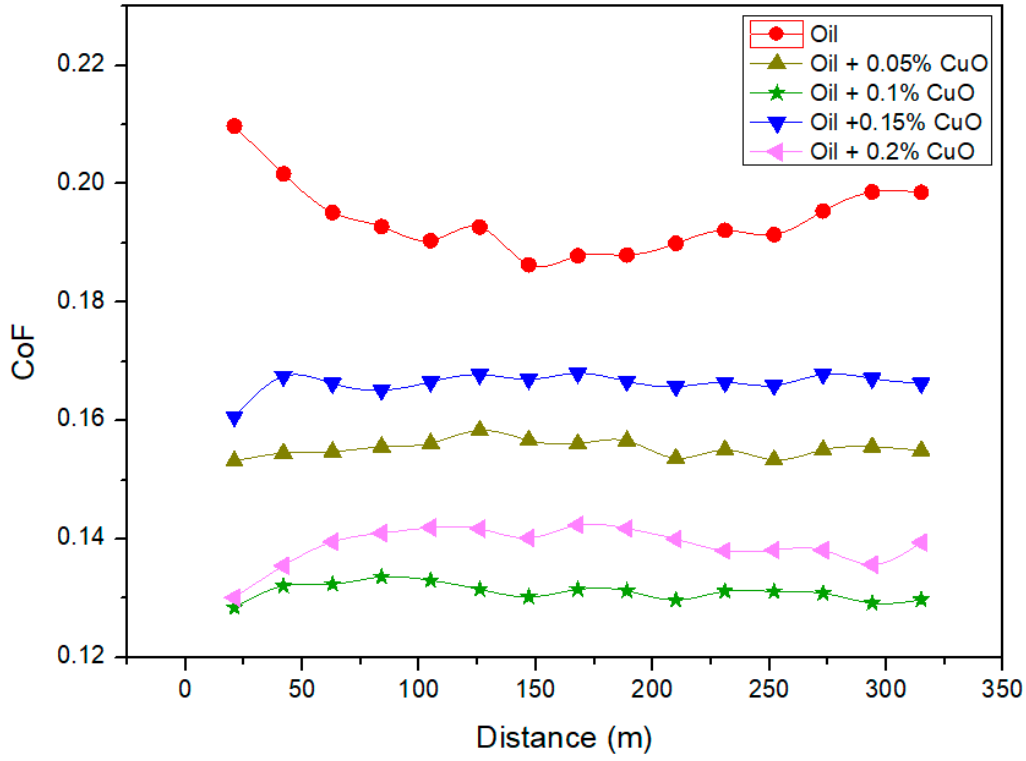


**Figure 15.** COF of pure oil and nanolubricants.

It is noteworthy that the maximum reduction in COF observed in our study is approximately 2.3 times higher than the maximum reduction reported by Peña-Parás et al. [23] for CuO nanoparticles. This difference can be attributed to the size and shape of the CuO material used as an additive. Peña-Parás et al. [23] utilized spherical CuO nanopartcles, whereas

we utilized CuO nanoplatelets. Nanoplatelets render more surface area in contact with lubricating oil and slide easily when compressed as compared to spherical nanoparticles thereby showing a significant reduction in COF.

For further examination of wear tracks, the obtained wear tracks on the AISI 1045 steel reciprocating plate of each test using different nanolubricants were examined using SEM. Figure 16a–d shows an SEM image of the surfaces of wear tracks of different nanolubricants having 0.05%, 0.1%, 0.15%, and 0.2% concentrations of CuO NPs. Among all the track results, the track in the case of 0.1% concentration of CuO NPs showed a smoother surface. EDS of the wear track shown in Figure 16e depicts that there is no deposition of CuO NPs over the wear track. The reduction in COF and smoother surface (low wear) was obtained due to the formation of tribo-film between the two surfaces as shown in Figure 17, high dispersion quality, and good bonding between the NPs and the lubricating oil that carries CuO NPs between the two surfaces.

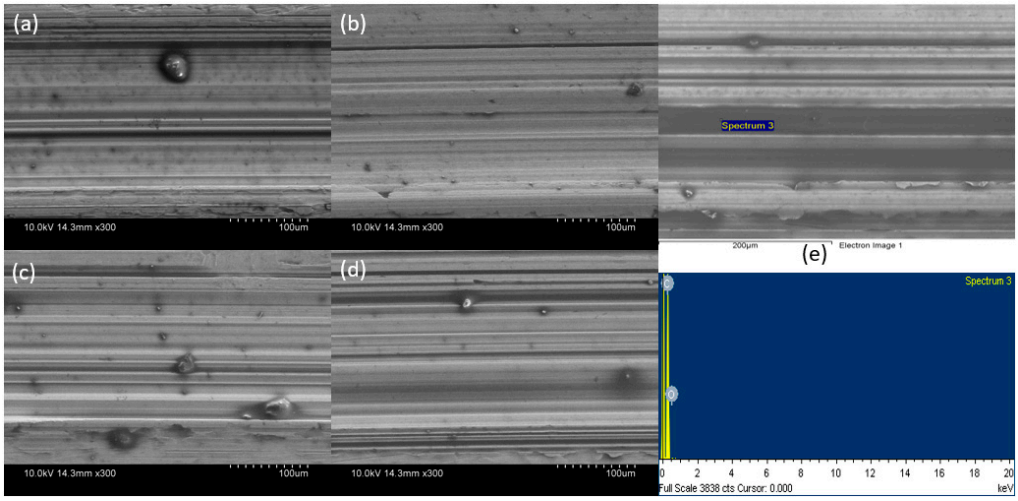


**Figure 16.** SEM image of wear track for (**a**) 0.05, (**b**) 0.1, (**c**) 0.15, and (**d**) 0.2 weight percent concentration of CuO NPs; (**e**) EDS of wear surface.

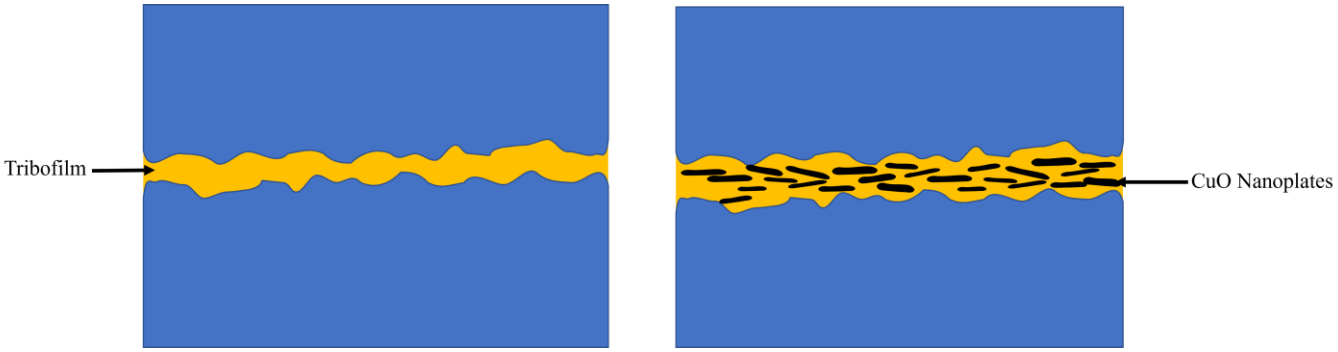


**Figure 17.** Schematic representation of the formation of tribofilm.

To augment the findings derived from SEM images, a high-speed confocal laser scanning microscope (Nanoscop NS-3500) was employed to conduct roughness analysis. This advanced instrument facilitates the generation of both 3D and 2D surface profiles for the target surface. The roughness parameters extracted from the microscope include maximum mean height (Ra), root mean square deviation (Rq), skewness (Rsk), kurtosis (Rk), maximum peak height (Rp), maximum profile valley depth (Rv), and the total height of the profile (Rt). Sahin M. et al. [42] investigated the effect of surface roughness on the frictional properties of different materials and conditions and Tian S.F. et al. [43] results showed that with the change of surface roughness changes under which the

friction coefficient and wear rate change. Figure 18 presents the 3D and 2D profiles of the plate surface, both before and after sanding, while Figure 19 showcases a comparison of the roughness parameters extracted from the plate surface pre- and post-sanding, revealing the improved surface quality after sanding. Additionally, Figure 20 displays the 3D and 2D profiles of the wear tracks, and Figure 21 highlights the comparison of roughness parameters across all wear tracks. Notably, the wear track treated with 0.1 wt% concentration of nanolubricant exhibits the most favorable results, consistent with the earlier findings obtained from the tribometer analysis.

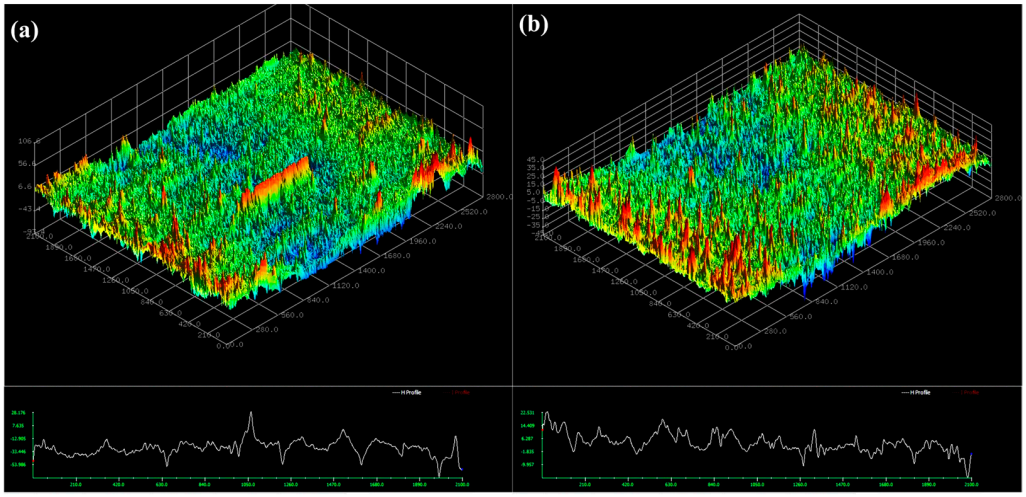


**Figure 18.** The surface profile of plate (**a**) before sanding (**b**) after sanding.

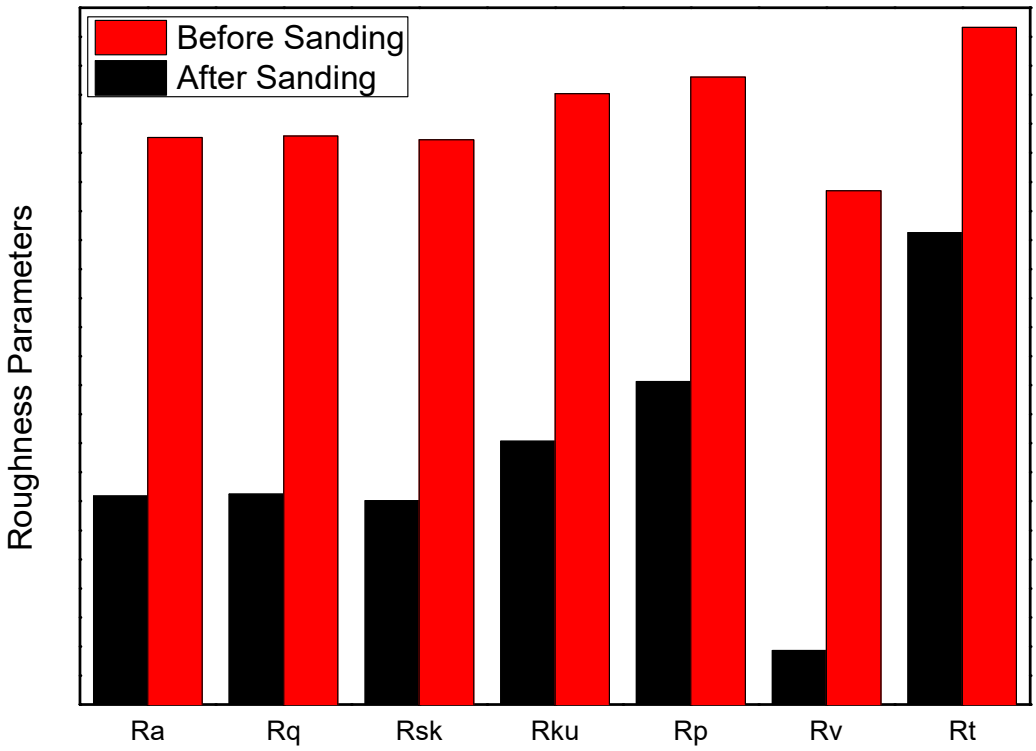


**Figure 19.** Roughness parameters comparing before sanding and after sanding.

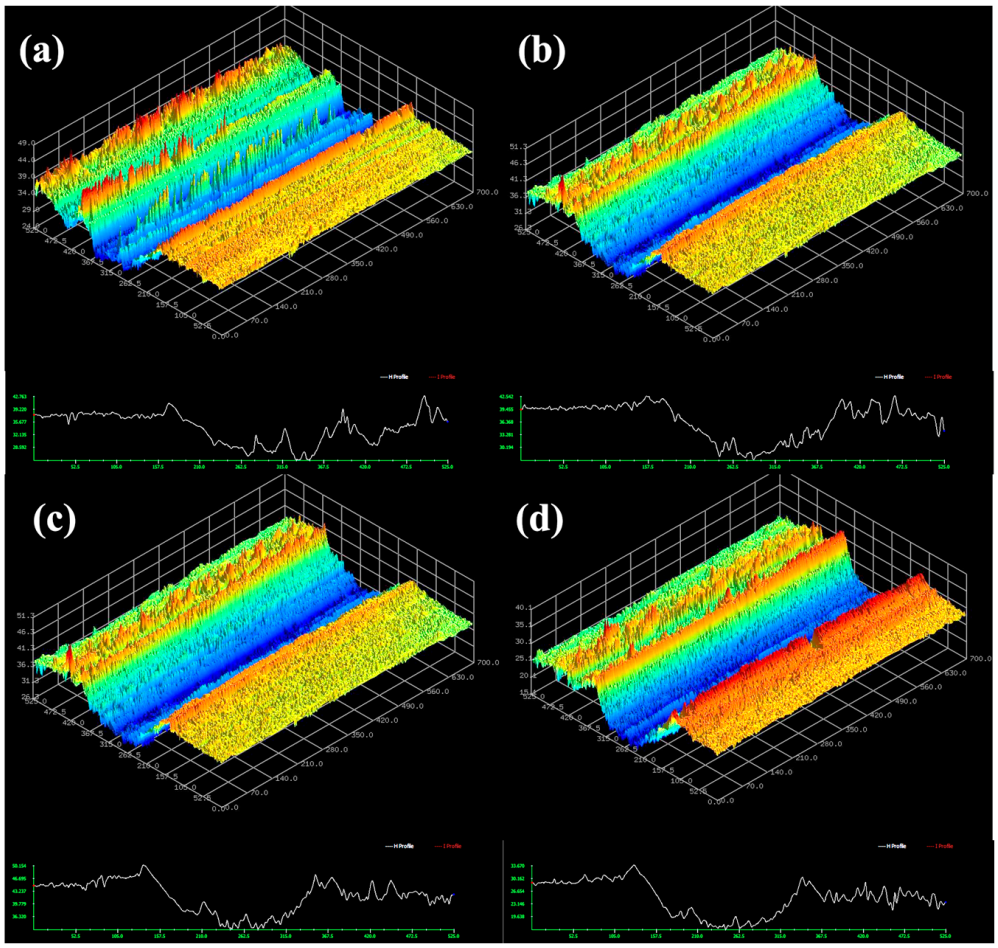


**Figure 20.** The surface profile of wear tracks from (**a**) 0.05, (**b**) 0.1, (**c**) 0.15, and (**d**) 0.2 wt% concentrations.

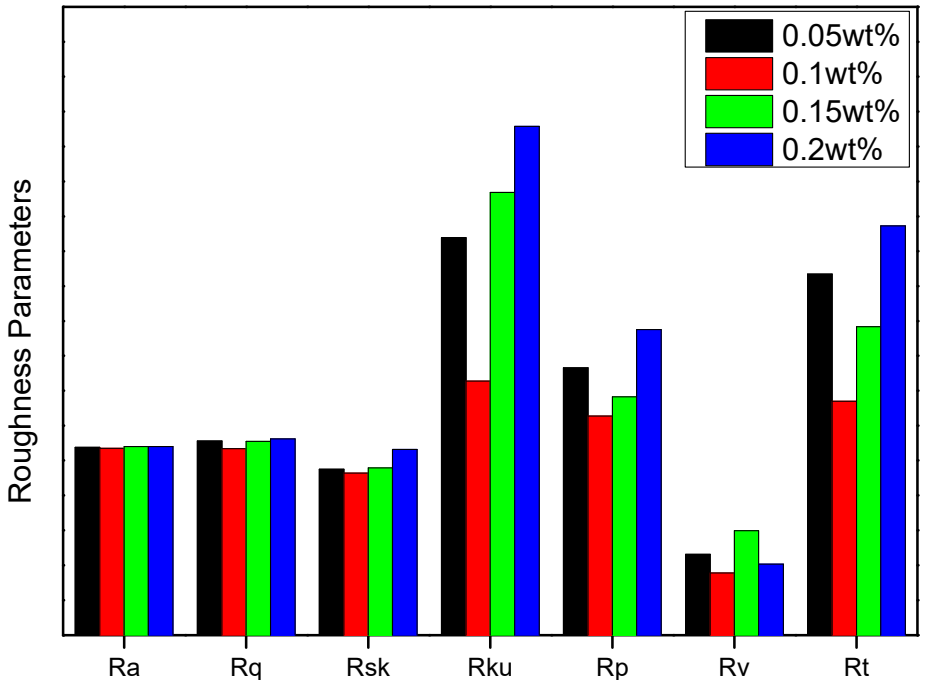


**Figure 21.** Roughness parameters comparing all the wear tracks.

## 4. Conclusions

The conclusion of the study is summarized in the following points:

- CuO nanoparticles were successfully synthesized using the sonochemical method and characterized using various techniques. The nanoparticles exhibited plate shapes which can be achieved using the sonochemical method.
- A reciprocating tribometer was designed and fabricated to measure the coefficient of friction (COF) of nanolubricants.
- Nanolubricants were prepared by varying the weight percent concentrations of CuO nanoparticles, and a 0.1% concentration of CuO nanoparticles as an additive in lubricating oil exhibited the lowest COF. The reduction in COF was 32% compared to pure synthetic oil.
- SEM and FE-TEM analyses confirmed the formation of a tribo-film over the CuO nanoparticles, which played a significant role in reducing the COF.
- Zeta potential measurements verified the good quality dispersion of 0.1% concentration of CuO nanoparticles as an additive in the lubricating oil.
- Wear track visual analysis using SEM demonstrated the best results for 0.1% concentration.
- The analysis of roughness parameters corroborates the findings obtained from tribometers and SEM analysis.
- The study suggests that a 0.1% concentration of CuO nanoparticles is the optimized value for using them as an additive in fully synthetic motor oil (SEA 5W-40).
- The findings of this study suggest the promising application of synthesized CuO nanoparticles as an additive in a commercially available fully synthetic lubricating oil (SEA 5W-40) to enhance its tribological properties.
- Advanced lubrication using CuO nanoparticles as additives has the potential to enhance the efficiency and lifespan of machines, and consequently reduce energy demand.

**Author Contributions:** Conceptualization, S.A. and S.-S.P.; methodology, S.A. and S.-S.P.; writing—original draft preparation, S.A.; supervision, S.-S.P.; funding acquisition, S.-S.P. All authors have read and agreed to the published version of the manuscript.

**Funding:** This work was supported by the 2022 Yeungnam University Research Grant.

**Data Availability Statement:** The data presented in this study are available on request from the corresponding author. The data are not publicly available due to privacy.

**Conflicts of Interest:** The authors declare no conflict of interest.

## References

1. Zhou, J.; Wu, Z.; Zhang, Z.; Liu, W.; Xue, Q. Tribological behavior and lubricating mechanism of Cu nanoparticles in oil. *Tribol. Lett.* **2000**, *8*, 213–218. [CrossRef]
2. Kreivaitis, R.; Gumbytė, M.; Kupčinskas, A.; Kazancev, K.; Ta, T.N.; Horng, J.H. Investigation of tribological properties of two protic ionic liquids as additives in water for steel–steel and alumina–steel contacts. *Wear* **2020**, *456–457*, 203390. [CrossRef]
3. Xiong, S.; Liang, D.; Kong, F. Effect of pH on the Tribological Behavior of Eu-Doped $WO_3$ Nanoparticle in Water-Based Fluid. *Tribol. Lett.* **2020**, *68*, 126. [CrossRef]
4. Du, Y.; Zhang, Z.; Wang, D.; Zhang, L.; Cui, J.; Chen, Y.; Wu, M.; Kang, R.; Lu, Y.; Yu, J.; et al. Enhanced tribological properties of aligned graphene-epoxy composites. *Friction* **2022**, *10*, 854–865. [CrossRef]
5. Guegan, J.; Southby, M.; Spikes, H. Friction Modifier Additives, Synergies and Antagonisms. *Tribol. Lett.* **2019**, *67*, 83. [CrossRef]
6. Shenoy, B.S.; Binu, K.G.; Pai, R.S.; Rao, D.S.; Pai, R.S. Effect of nanoparticles additives on the performance of an externally adjustable fluid film bearing. *Tribol. Int.* **2012**, *45*, 38–42. [CrossRef]
7. Zhao, J.; Yang, G.; Zhang, Y.; Zhang, S.; Zhang, C.; Gao, C.; Zhang, P. Controllable synthesis of different morphologies of CuO nanostructures for tribological evaluation as water-based lubricant additives. *Friction* **2021**, *9*, 963–977. [CrossRef]
8. Abdel-Rehim, A.A.; Akl, S.; Elsoudy, S. Investigation of the tribological behavior of mineral lubricant using copper oxide nano additives. *Lubricants* **2021**, *9*, 16. [CrossRef]
9. Shafi, W.K.; Charoo, M.S. An overall review on the tribological, thermal and rheological properties of nanolubricants. *Tribol.—Mater. Surf. Interfaces* **2021**, *15*, 20–54. [CrossRef]
10. Huang, S.; Wang, Z.; Xu, L.; Huang, C. Friction and Wear Characteristics of Aqueous $ZrO_2$/GO Hybrid Nanolubricants. *Lubricants* **2022**, *10*, 109. [CrossRef]

11. Dembelova, T.; Badmaev, B.; Makarova, D.; Mashanov, A.; Mishigdorzhiyn, U. Rheological and Tribological Study of Polyethylsiloxane with $SiO_2$ Nanoparticles Additive. *Lubricants* **2022**, *11*, 9. [CrossRef]
12. Trivedi, K. Analyzing lubrication properties of magnetic lubricant synthesized in two lubricating oils. *Wear* **2021**, *477*, 203861. [CrossRef]
13. Alqahtani, B.; Hoziefa, W.; Moneam, H.M.A.; Hamoud, M.; Salunkhe, S.; Elshalakany, A.B.; Abdel-Mottaleb, M.; Davim, J.P. Tribological Performance and Rheological Properties of Engine Oil with Graphene Nano-Additives. *Lubricants* **2022**, *10*, 137. [CrossRef]
14. Rylski, A.; Siczek, K. The Effect of Addition of Nanoparticles, Especially $ZrO_2$-Based, on Tribological Behavior of Lubricants. *Lubricants* **2020**, *8*, 23. [CrossRef]
15. Szabó, Á.I.; Tóth, Á.D.; Leskó, M.Z.; Hargitai, H. Investigation of the Applicability of $Y_2O_3$–$ZrO_2$ Spherical Nanoparticles as Tribological Lubricant Additives. *Lubricants* **2022**, *10*, 152. [CrossRef]
16. Padgurskas, J.; Rukuiza, R.; Prosyčevas, I.; Kreivaitis, R. Tribological properties of lubricant additives of Fe, Cu and Co nanoparticles. *Tribol. Int.* **2013**, *60*, 224–232. [CrossRef]
17. Prabu, L.; Saravanakumar, N.; Rajaram, G. Influence of Ag Nanoparticles for the Anti-wear and Extreme Pressure Properties of the Mineral Oil Based Nano-cutting Fluid. *Tribol. Ind.* **2018**, *40*, 440–447. [CrossRef]
18. Shahnazar, S.; Bagheri, S.; Abd Hamid, S.B. Enhancing lubricant properties by nanoparticle additives. *Int. J. Hydrogen Energy* **2016**, *41*, 3153–3170. [CrossRef]
19. Laad, M.; Jatti, V.K.S. Titanium oxide nanoparticles as additives in engine oil. *J. King Saud Univ.—Eng. Sci.* **2018**, *30*, 116–122. [CrossRef]
20. Dai, W.; Kheireddin, B.; Gao, H.; Liang, H. Roles of nanoparticles in oil lubrication. *Tribol. Int.* **2016**, *102*, 88–98. [CrossRef]
21. Alves, S.M.; Mello, V.S.; Faria, E.A.; Camargo, A.P.P. Nanolubricants developed from tiny CuO nanoparticles. *Tribol. Int.* **2016**, *100*, 263–271. [CrossRef]
22. Gulzar, M.; Masjuki, H.; Varman, M.; Kalam, M.; Mufti, R.A.; Zulkifli, N.; Yunus, R.; Zahid, R. Improving the AW/EP ability of chemically modified palm oil by adding CuO and $MoS_2$ nanoparticles. *Tribol. Int.* **2015**, *88*, 271–279. [CrossRef]
23. Peña-Parás, L.; Taha-Tijerina, J.; Garza, L.; Maldonado-Cortés, D.; Michalczewski, R.; Lapray, C. Effect of CuO and $Al_2O_3$ nanoparticle additives on the tribological behavior of fully formulated oils. *Wear* **2015**, *332–333*, 1256–1261. [CrossRef]
24. Hernández Battez, A.; González, R.; Viesca, J.L.; Fernández, J.E.; Díaz Fernández, J.M.; Machado, A.; Chou, R.; Riba, J. CuO, $ZrO_2$ and ZnO nanoparticles as antiwear additive in oil lubricants. *Wear* **2008**, *265*, 422–428. [CrossRef]
25. Gupta, R.N.; Harsha, A.P. Tribological study of castor oil with surface-modified CuO nanoparticles in boundary lubrication. *Ind. Lubr. Tribol.* **2018**, *70*, 700–710. [CrossRef]
26. Thottackkad, M.V.; Rajendrakumar, P.K.; Prabhakaran Nair, K. Experimental studies on the tribological behaviour of engine oil (SAE15W40) with the addition of CuO nanoparticles. *Ind. Lubr. Tribol.* **2014**, *66*, 289–297. [CrossRef]
27. Bhaumik, S.; Pathak, S.D. Analysis of anti-wear properties of cuo nanoparticles as friction modifiers in mineral oil (460cst viscosity) using pin-on-disk tribometer. *Tribol. Ind.* **2015**, *37*, 196–203.
28. Salguero, J.; Vazquez-Martinez, J.; Sol, I.; Batista, M. Application of Pin-On-Disc Techniques for the Study of Tribological Interferences in the Dry Machining of A92024-T3 (Al–Cu) Alloys. *Materials* **2018**, *11*, 1236. [CrossRef]
29. Velkavrh, I.; Lüchinger, M.; Kern, K.; Klien, S.; Ausserer, F.; Voyer, J.; Diem, A.; Schreiner, M.; Tillmann, W. Using a standard pin-on-disc tribometer to analyse friction in a metal forming process. *Tribol. Int.* **2017**, *114*, 418–428. [CrossRef]
30. Jackson, C.L.; Mosley, D.W. Model Friction Studies of Chemical Mechanical Planarization Using a Pin-on-Disk Tribometer. *Tribol. Lett.* **2019**, *67*, 81. [CrossRef]
31. Hernández Battez, A.; González, R.; Felgueroso, D.; Fernández, J.E.; del Rocío Fernández, M.; García, M.A.; Peñuelas, I. Wear prevention behaviour of nanoparticle suspension under extreme pressure conditions. *Wear* **2007**, *263*, 1568–1574. [CrossRef]
32. Chenga Reddy, P.; Arumugam, S.; Nithin Sai Krishna, P.; Jaya Sainath, N. Tribological investigation of a compressor liner-ring material under various bio-based lubricants using HFRR tribometer. *IOP Conf. Ser. Mater. Sci. Eng.* **2018**, *390*, 012025. [CrossRef]
33. Balakumar, R.; Sriram, G.; Arumugam, S. Assessment on Tribological Characteristics of Waste Ayurvedic Oil Biodiesel Blends using High-Frequency Reciprocating Rig Tribometer. *IOP Conf. Ser. Mater. Sci. Eng.* **2018**, *390*, 012047. [CrossRef]
34. Shahsavani, E.; Feizi1, N.; Khalaji, A.D. Copper oxide nanoparticles by solid-state thermal decomposition: Synthesis and characterization. *J. Ultrafine Grained Nanostruct. Mater.* **2016**, *49*, 48–50.
35. Dagher, S.; Haik, Y.; Ayesh, A.I.; Tit, N. Synthesis and optical properties of colloidal CuO nanoparticles. *J. Lumin.* **2014**, *151*, 149–154. [CrossRef]
36. Kumaresan, N.; Ramamurthi, K.; Mathuri, S.; Maria Angelin Sinthiya, M.; Manimozhi, T.; Margoni, M.M.; Rameshbabu, R. Solid state synthesis of Cuo nanoparticles for photo catalytic application. *Int. J. ChemTech. Res.* **2015**, *7*, 1598–1602.
37. Kayani, Z.N.; Umer, M.; Riaz, S.; Naseem, S. Characterization of Copper Oxide Nanoparticles Fabricated by the Sol–Gel Method. *J. Electron. Mater.* **2015**, *44*, 3704–3709. [CrossRef]
38. Azam, A. Size-dependent antimicrobial properties of CuO nanoparticles against Gram-positive and -negative bacterial strains. *Int. J. Nanomed.* **2012**, *7*, 3527. [CrossRef]
39. Chen, Y.; Renner, P.; Liang, H. Dispersion of Nanoparticles in Lubricating Oil: A Critical Review. *Lubricants* **2019**, *7*, 7. [CrossRef]
40. Kumar, A.; Dixit, C.K. Methods for characterization of nanoparticles. In *Advances in Nanomedicine for the Delivery of Therapeutic Nucleic Acids*; Elsevier: Amsterdam, The Netherlands, 2017; pp. 43–58; ISBN 9780081005576.

41. Joly-Pottuz, L.; Vacher, B.; Ohmae, N.; Martin, J.M.; Epicier, T. Anti-wear and friction reducing mechanisms of carbon nano-onions as lubricant additives. *Tribol. Lett.* **2008**, *30*, 69–80. [CrossRef]
42. Sahin, M.; Çetinarslan, C.S.; Akata, H.E. Effect of surface roughness on friction coefficients during upsetting processes for different materials. *Mater. Des.* **2007**, *28*, 633–640. [CrossRef]
43. Tian, S.F.; Jiang, L.T.; Guo, Q.; Wu, G.H. Effect of surface roughness on tribological properties of $TiB_2$/Al composites. *Mater. Des.* **2014**, *53*, 129–136. [CrossRef]